Strong Correlation of Electronic and Lattice Excitations in GaAs/AlGaAs Semiconductor Quantum Wells Revealed by Two-Dimensional Terahertz Spectroscopy

W. Kuehn,[1] K. Reimann,[1] M. Woerner,[1,*] T. Elsaesser,[1] R. Hey,[2] and U. Schade[3]

[1]*Max-Born-Institut für Nichtlineare Optik und Kurzzeitspektroskopie, 12489 Berlin, Germany*

[2]*Paul-Drude-Institut für Festkörperelektronik, 10117 Berlin, Germany*

[3]*Helmholtz-Zentrum Berlin für Materialien und Energie, 12489 Berlin, Germany*

(Received 7 January 2011; published 3 August 2011)

Coulomb-mediated interactions between intersubband excitations of electrons in GaAs/AlGaAs double quantum wells and longitudinal optical phonons are studied by two-dimensional spectroscopy in the terahertz frequency range. The multitude of diagonal and off-diagonal peaks in the 2D spectrum gives evidence of strong polaronic signatures in the nonlinear response. A quantitative theoretical analysis reveals a dipole coupling of electrons to the polar lattice that is much stronger than in bulk GaAs, due to a dynamic localization of the electron wave function by scattering processes.

DOI: 10.1103/PhysRevLett.107.067401 PACS numbers: 78.67.De, 71.38.Fp, 78.30.Fs, 78.47.jf

The coupling of electronic excitations to the crystal lattice plays a decisive role for the optical and transport properties of solids. In semiconductors, the spectra of both inter- and intraband optical transitions are strongly influenced by electron-phonon interactions [1]. Coupling to acoustic phonons causes spectral sidebands of exciton emission lines in, e.g., quantum dot (QD) systems [2,3]. The shapes of QD absorption and emission lines are strongly influenced by dephasing processes originating from second order interactions with optical [4] and acoustic phonons [5]. Electron-LO phonon coupling is highly relevant also for transport processes such as nonresonant tunneling in quasi-two-dimensional quantum well [6] and quantum cascade structures [7].

The Coulomb-mediated interaction of electrons with a polar lattice results in the formation of Fröhlich polarons which are quasiparticles consisting of an electron and a surrounding cloud of LO phonons [8]. Polaronic signatures have been found both in charge transport as a quantum kinetic phenomenon [9] and for low-energy excitations in low-dimensional semiconductors such as intersubband (IS) [10] and/or magneto-optical transitions [11]. Femtosecond pump-probe experiments have provided evidence for LO phonon sidebands of IS transitions in a GaN/AlGaN heterostructure [12].

The coupling strength of electronic dipoles to a polar lattice depends on both the lattice polarity and the spatial extension of the electron wave function. A *static* quantum confinement of electrons in two or less dimensions and/or electron localization in disorder potentials enhances the electronic polarization (dipole density) and, thus, the electron-LO phonon coupling. A *dynamic* enhancement can arise when the electron wave function undergoes a transient localization by scattering processes. The latter phenomenon has remained mainly unaddressed, partly due to the lack of sensitive experimental probes of the interaction strength. While linear optical spectra reflect electron-phonon coupling, it is difficult to extract quantitative information because the line shapes are also influenced by other broadening mechanisms, e.g., by Coulomb correlations. Ultrafast pump-probe experiments give insight into carrier dynamics, but the strength of electron-phonon coupling can be estimated only indirectly.

The more sophisticated technique of nonlinear two-dimensional spectroscopy expands the nonlinear response of the system along two independent frequency coordinates and separates different couplings via characteristic cross peaks in the 2D spectrum. Both heterodyne detected photon echoes [13–15] and a novel method of collinear 2D spectroscopy in the terahertz range [16,17] bear the potential to analyze polaronic effects and electron-phonon coupling strengths in a quantitative way.

In this Letter, we study the fundamental interaction of large electronic IS dipoles with LO phonon excitations by collinear 2D THz spectroscopy of coupled GaAs/AlGaAs quantum wells (QWs) with subband energy spacings tailored to be close to the LO phonon energy. We demonstrate for the first time a strong polaronic coupling which governs the nonlinear IS response and dominates over Coulomb correlations of the IS dipoles. From the IS 2D spectrum, we quantitatively derive a dipole-dipole coupling between the IS excitation and LO phonons much stronger than the electron-LO phonon coupling in bulk GaAs. The large coupling strength is due to dynamic localization effects in the electron wave function.

The sample studied here was grown by molecular beam epitaxy and processed into a prism shape. It consists of coupled GaAs QWs of 9 and 12 nm width, separated by 2-nm-thick $Al_{0.35}Ga_{0.65}As$ barriers. The nine pairs of coupled QWs are separated by 15-nm-thick $Al_{0.35}Ga_{0.65}As$ barriers, the centers of which are doped with Si, resulting in an electron concentration of $n_s = 1 \times 10^{12}$ cm^{-2} per pair. According to a $k \cdot p$ band structure calculation, the sample has bound states in the wide well (WW) at

$E_1 = 0$, $E_3 = 70$ meV, and $E_5 = 157$ meV and in the narrow well (NW) at $E_2 = 12$ meV and $E_4 = 116$ meV [Fig. 1(a)]. At $T = 300$ K subbands E_1 and E_2 are thermally populated.

Linear absorption spectra for temperatures of 10 and 300 K were measured by Fourier transform spectroscopy. In the range from 2 to 17 THz we used THz radiation from a synchrotron and a liquid helium-cooled Si bolometer, in the range from 17 to 60 THz thermal emission from a globar and a liquid nitrogen-cooled HgCdTe detector. Since the IS dipoles interact only with p-polarized light, we referenced the p-polarized to the s-polarized spectrum

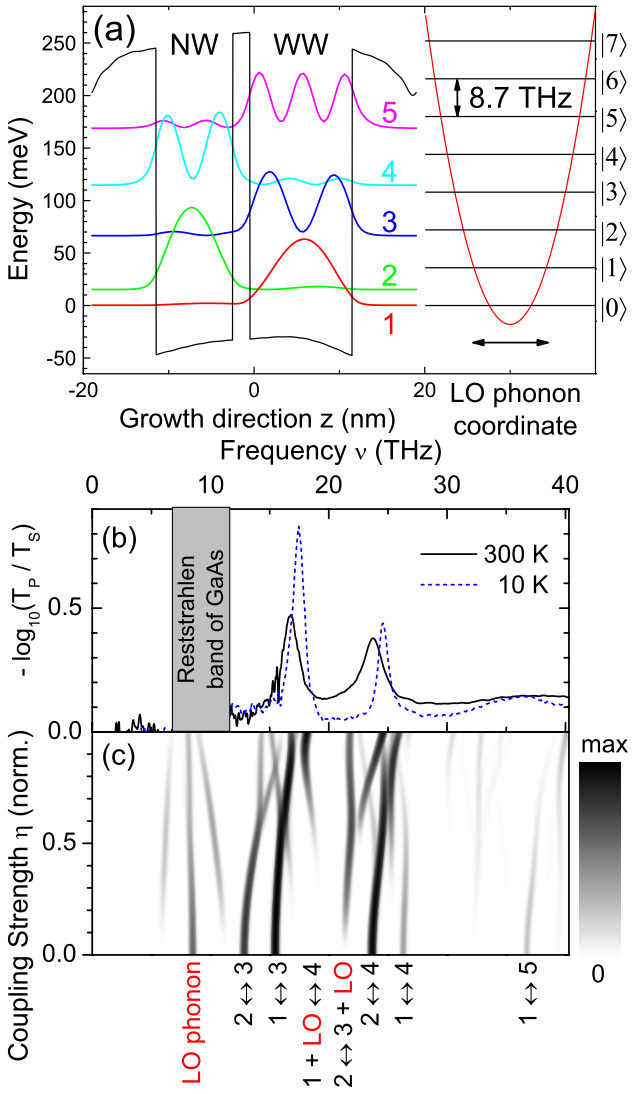

FIG. 1 (color online). (a) Potential energy and $|\Psi_n(x)|^2$ for the five lowest subbands of two coupled AlGaAs/GaAs quantum wells and schematic of LO phonon states separated by $\nu_{LO} = 8.7$ THz. (b) Linear IS absorption spectra for lattice temperatures of 10 and 300 K. (c) Calculated IS absorption spectra as a function of the electron-phonon coupling strength η [19]. A smaller line width was chosen to visualize the electron-phonon coupling mechanism.

to determine the IS absorbance $A = -\log_{10}(T_P/T_S)$. The absorption spectra display two major IS transitions $1 \leftrightarrow 3$ at 17 THz ($\Delta E = 70$ meV) and $2 \leftrightarrow 4$ at 24 THz [$\Delta E = 99$ meV, Fig. 1(b)], matching the calculated fundamental transitions of the two QWs.

In the nonlinear experiment, the output from a femtosecond multipass amplifier is split and sent into two GaSe crystals to generate two phase-locked THz pulses A and B [pulse duration ≈ 100 fs, for spectra see Fig. 2(a)] by difference frequency mixing [18]. The two pulses with a mutual delay τ interact with the QW sample. The transmitted light is measured in amplitude and (absolute) phase by electro-optic sampling. Two choppers synchronized to the pulse repetition rate allow for measuring the electric-field transients $F_{AB}(t, \tau)$ (both pulses A and B are incident on the sample), $F_A(t)$ (only pulse A), and $F_B(t, \tau)$ (only pulse B). The nonlinear signal emitted from the sample is the difference $F_{NL}(t, \tau) = F_{AB}(t, \tau) - F_A(t) - F_B(t, \tau)$ and depends on the delay τ and the real time t. After a 2D Fourier transform of $F_{NL}(t, \tau)$ different time orderings and 2D frequency positions allow for identifying 6 different signal contributions (cf. Table 1 and Figs. 3 and 4 of [17]). Four of them are combined into a purely absorptive 2D correlation spectrum [waiting (population) time zero] as a function of ν_1 and ν_3, the excitation and detection frequencies.

In Fig. 2(a), we present the 2D correlation spectrum of the sample measured with electric-field amplitudes of the two THz pulses of 70 and 90 kV/cm. The third-order nonlinear signal is plotted as a function of ν_1 and ν_3. Positive signals correspond to an increase of sample transmission, negative signals to a decrease. The 2D spectrum displays several—partly overlapping—peaks on the diagonal and a variety of off-diagonal peaks. The diagonal signal includes peaks at the positions of the two IS absorption lines and between them, as is evident from the cross section along the diagonal of the 2D spectrum [green line in Fig. 3(a)]. The signals show strong cross peaks with each other and with the $1 \leftrightarrow 3$ and $2 \leftrightarrow 4$ transitions. The red and blue dashed lines in Fig. 3(a) show cross sections along the detection frequency ν_3 at excitation frequencies ν_1 resonant to the $1 \leftrightarrow 3$ and $2 \leftrightarrow 4$ transitions.

In Figs. 3(b) and 3(c), we show pump-probe data taken with pulse B as the pump on the $1 \leftrightarrow 3$ transition and pulse A as a broadband probe. The transient IS spectra [Fig. 3(b)] exhibit a small instantaneous bleaching on the $1 \leftrightarrow 3$ transition at 18 THz and a transmission decrease around $\nu_3 = 21$ THz, probably due to an enhanced $3 \leftrightarrow 5$ absorption. The onset of the strong transmission increase at 24 THz shows a delay of ≈ 100 fs corresponding to the LO phonon period. This contribution is due to stimulated emission in the narrow QW ($4 \leftrightarrow 2$ transition) after a phonon-mediated population transfer into subband 4 (lifetime 3 ps). Time resolved data taken at a fixed detection frequency of $\nu_3 = 23$ THz [Fig. 3(c)] display strong oscillations with

$\nu_{LO} = 8.7$ THz, pointing to quantum beats involving LO phonon sidebands.

We now discuss the nonlinear IS response. The pump-probe data [Figs. 3(b) and 3(c)] display pronounced phonon-related signatures such as the delayed onset of $4 \leftrightarrow 2$ stimulated emission at $\nu_3 = 24$ THz and the oscillatory time evolution at 23 THz. Considering the energy positions of the different QW subbands and the LO phonon quantum states [Fig. 1(a)], one finds subband and phonon states which are close to energetic resonance. This fact together with the polar optical interaction of electrons with the GaAs lattice results in a pronounced coupling of IS and LO phonon excitations, i.e., polaronic signatures in the ultrafast nonlinear IS response. Much richer information gives the 2D correlation spectrum [Fig. 2(a)]. The diagonal peaks due to the fundamental $1 \leftrightarrow 3$ and $2 \leftrightarrow 4$ transitions are complemented by other contributions of similar strengths [Fig. 3(a)]. The absence of cross peaks of the $1 \leftrightarrow 3$ and $2 \leftrightarrow 4$ transitions (not sharing a common level) shows that the coupling of IS dipoles located in neighboring QWs is much smaller than their coupling to LO phonons. The latter gives rise to the additional diagonal and to the rich variety of off-diagonal peaks.

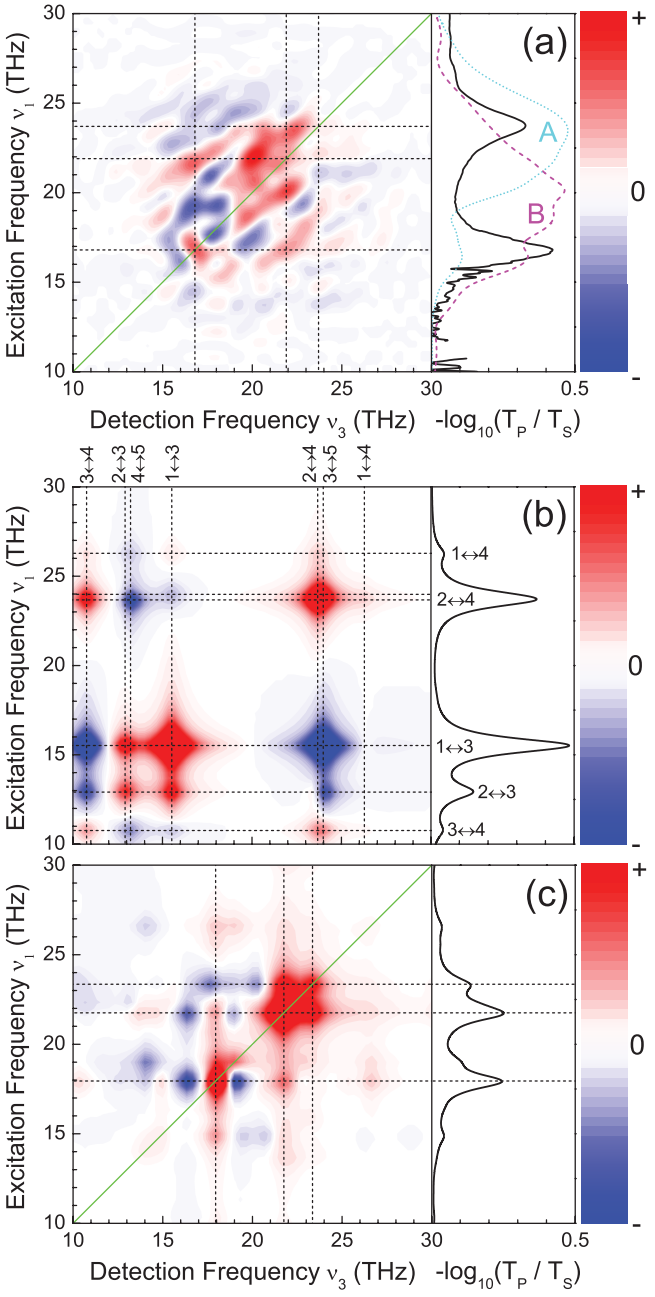

FIG. 2 (color). (a) Measured 2D correlation spectrum as a function of the excitation frequency ν_1 and detection frequency ν_3. One observes strong signals along the excitation frequency ν_1 between the major IS absorption lines due to the polaronic nature of IS transitions. Solid and dashed lines indicate the sections shown in Fig. 3(a). (b) Calculated 2D spectrum of the undressed ($\eta = 0$) electronic IS oscillator. (c) Calculated spectrum of the dressed oscillator ($\eta \approx 1$), showing polaronic signatures. Right panels: Measured (a) and calculated (b), (c) linear IS absorption. In (a) the spectra of pulses A and B are shown.

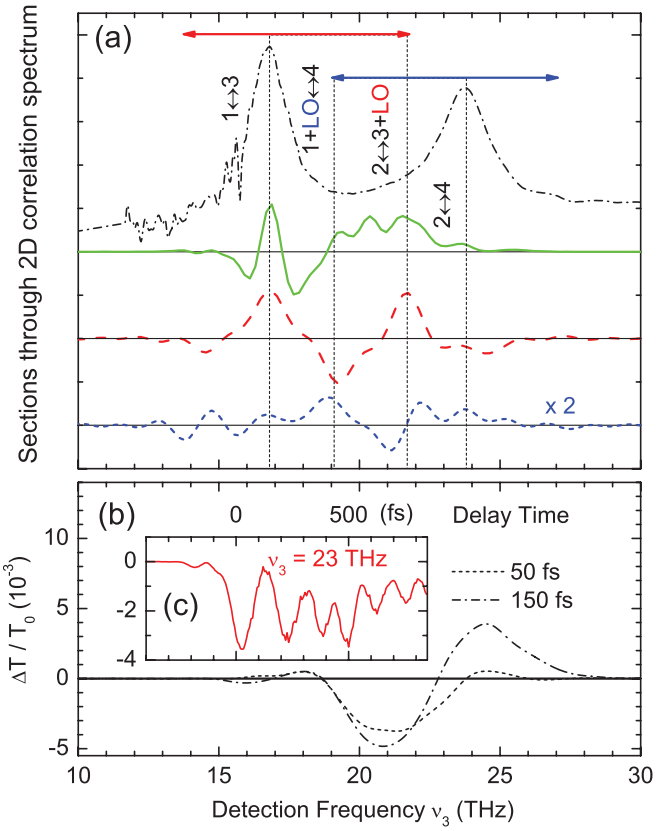

FIG. 3 (color). (a) Cross sections through the measured 2D correlation spectrum [Fig. 2(a)]. Green solid line: signal along the diagonal; red (blue) dashed lines: cross sections for ν_1 resonant to the $1 \leftrightarrow 3$ ($2 \leftrightarrow 4$) transition, respectively. (b) Spectrally resolved transmission changes induced by the 19 THz centered pump pulse for two different delays of the probe pulses. (c) Time transient at $\nu_3 = 23$ THz where pronounced oscillations with the LO frequency occur.

To analyze such a coupling scenario in more detail, we performed theoretical calculations. We construct a Hamiltonian in the direct product space of the electronic subband levels and one prominent LO phonon mode:

$$H = H^0_{\mathrm{IS}} \otimes I_{\mathrm{LO}} + I_{\mathrm{IS}} \otimes H^0_{\mathrm{LO}} - (D_{\mathrm{IS}} \otimes I_{\mathrm{LO}} + I_{\mathrm{IS}} \otimes D_{\mathrm{LO}})F(t) + \eta(D_{\mathrm{IS}} \otimes I_{\mathrm{LO}})(I_{\mathrm{IS}} \otimes D_{\mathrm{LO}}). \quad (1)$$

H^0_{IS} and H^0_{LO} are the unperturbed Hamiltonians, I^0_{IS} and I^0_{LO} the identity operators of the respective Hilbert space, and D^0_{IS} and D^0_{LO} are the electric dipole operators of the IS transition and the phonon oscillator, respectively. The second term describes the coupling to the electromagnetic field and the last term stands for an electric dipole-dipole interaction between the IS and LO phonon transition dipoles with a coupling strength η [19]. Assuming that all transitions between thermally populated levels are homogeneously broadened with a common dephasing time T_2, the linear absorption spectrum $A(\nu)$ and the 2D correlation spectrum $S(\nu_1, \nu_3)$ at a waiting time zero read as follows:

$$A(\nu) = C_A \sum_{i,j} N_i(T) d^2_{ij} \nu_{ij} g(\nu - \nu_{ij}), \quad (2)$$

$$S(\nu_1, \nu_3) = C_S \sum_{i,j,k} N_i(T) d^2_{ij} g(\nu_1 - \nu_{ij})[d^2_{ik} \nu_{ik} g(\nu_3 - \nu_{ik}) - d^2_{jk} \nu_{jk} g(\nu_3 - \nu_{jk})], \quad (3)$$

with

$$N_i(T) = \frac{e^{-\epsilon_i/k_B T}}{\sum_j e^{-\epsilon_i/k_B T}}$$

and

$$g(\nu) = \frac{1}{(2\pi\nu)^2 + T_2^{-2}}.$$

Here, the energy eigenstates ϵ_i, the transition dipoles d_{ij}, and the frequencies $h\nu_{i,j} = \epsilon_j - \epsilon_i$ depend sensitively on the dipole-dipole coupling parameter η.

Results for different values of η are presented in Figs. 1(c), 2(b), and 2(c). For $\eta = 0$ (no coupling), the electronic single particle picture predicts IS transitions at frequencies corresponding to the subband energy separations in Fig. 1(a). The linear absorption spectrum consists of two intrawell transitions ($1 \leftrightarrow 3$ and $2 \leftrightarrow 4$) and two tunneling assisted transitions $2 \leftrightarrow 3$ and $1 \leftrightarrow 4$ [Fig. 1(c)]. The corresponding 2D correlation spectrum [Fig. 2(b)] exhibits strong positive diagonal peaks for the $2 \leftrightarrow 3$, $1 \leftrightarrow 3$, and $2 \leftrightarrow 4$ IS transitions. Positive cross peaks (in red) at $(\nu_1, \nu_3) = (13, 15.5)$ and $(15.5, 13)$ THz are due to the coupling of the $2 \leftrightarrow 3$ and $1 \leftrightarrow 3$ transitions via the joint subband 3. Negative off-diagonal peaks (in blue) reflect transitions from excited subbands and/or enhanced absorption on transitions initially blocked by electron populations (state filling, Pauli blocking). Assignments of the negative peaks are indicated in Fig. 2(b). The calculated 2D spectrum in Fig. 2(b), however, does not reproduce the number and the spectral positions of the experimental 2D peaks in Fig. 2(a). Evidently, a single particle picture misses essential features of the nonlinear IS response.

With increasing coupling $0 < \eta \leq 1$, the calculated linear absorption and 2D spectra [Figs. 1(c) and 2(c)] develop distinct polaronic signatures. For $\eta \approx 1$, the spectral positions of the purely electronic transitions are shifted, due to the renormalized subband energies, and new phonon-assisted transitions occur, such as the prominent diagonal and cross peaks due to the $1 + \mathrm{LO} \leftrightarrow 4$ and $2 \leftrightarrow 3 + \mathrm{LO}$ transitions [Figs. 2(c) and 3(a)]. The $2 \leftrightarrow 3 + \mathrm{LO}$ peak at $\nu_1 = 22$ THz is an anti-Stokes phonon sideband giving rise to the quantum beat with $\nu_{\mathrm{LO}} = 8.7$ THz observed at $\nu_3 = 23$ THz in the spectrally resolved pump-probe measurements [Fig. 3(c)]. The 2D spectrum in Fig. 2(c) reproduces the main features and the renormalized energy scale of the experimental spectrum [Fig. 2(a)] and, thus, allows us to derive an interaction strength $\eta \approx 1$.

The strength of the dipole-dipole interaction η depends sensitively on the spatial extension Δx of the electron wave function in the QW plane [20]; the coupling increases with decreasing Δx. An electron wave packet with an in-plane extension given by the thermal de Broglie wavelength at $T = 300$ K, $\Delta x^2 = \hbar^2/4 m_{\mathrm{eff}} k_B T \approx (3.5)^2$ nm^2 and an IS dipole of $d_{\mathrm{IS}} = e_0 \times d_z \approx e_0 \times 10$ nm causes a polar interaction energy [20] of $H_{\mathrm{int}} \approx (\epsilon_\infty^{-1} - \epsilon_s^{-1}) e_0 d_{\mathrm{IS}} / (\epsilon_0 \Delta x^2) = 200$ meV, much larger than the binding energy $E_{\mathrm{trap}} \approx 5$ meV of the polaron in bulk GaAs [9]. At $T = 300$ K, in-plane electron localization via monolayer fluctuations of the QW thickness plays a minor role. However, the high scattering rates of electrons at $T = 300$ K limit Δx to the thermal de Broglie wavelength. This dynamic localization gives rise to the observed high coupling strength $\eta \approx 1$ [9,20,21].

In conclusion, nonlinear two-dimensional THz spectroscopy gives quantitative insight into the dipole-mediated coupling of electronic IS transitions and LO phonons in GaAs quantum wells. This coupling is manifested in strong polaronic features of the linear and nonlinear IS response. The enhancement of coupling strength by more than a factor of 10 compared to bulk GaAs is attributed to a dynamic in-plane localization of electrons.

*woerner@mbi-berlin.de

[1] R. E. Dietz, D. G. Thomas, and J. J. Hopfield, Phys. Rev. Lett. **8**, 391 (1962).
[2] E. Peter *et al.*, Phys. Rev. B **69**, 041307(R) (2004).
[3] L. Besombes, K. Kheng, L. Marsal, and H. Mariette, Phys. Rev. B **63**, 155307 (2001).
[4] A. V. Uskov *et al.*, Phys. Rev. Lett. **85**, 1516 (2000).
[5] E. A. Muljarov and R. Zimmermann, Phys. Rev. Lett. **93**, 237401 (2004).
[6] D. Y. Oberli *et al.*, Appl. Phys. Lett. **56**, 1239 (1990).

[7] M. Woerner, K. Reimann, and T. Elsaesser, J. Phys. Condens. Matter **16**, R25 (2004).
[8] H. Fröhlich, Adv. Phys. **3**, 325 (1954).
[9] P. Gaal *et al.*, Nature (London) **450**, 1210 (2007).
[10] S. Butscher, J. Förstner, I. Waldmüller, and A. Knorr, Phys. Status Solidi B **241**, R49 (2004).
[11] S. Hameau *et al.*, Phys. Rev. Lett. **83**, 4152 (1999).
[12] Z. Wang *et al.*, Phys. Rev. Lett. **94**, 037403 (2005).
[13] M. C. Asplund, M. T. Zanni, and R. M. Hochstrasser, Proc. Natl. Acad. Sci. U.S.A. **97**, 8219 (2000).
[14] X. Q. Li, T. H. Zhang, C. N. Borca, and S. T. Cundiff, Phys. Rev. Lett. **96**, 057406 (2006).
[15] K. W. Stone *et al.*, Science **324**, 1169 (2009).
[16] W. Kuehn, K. Reimann, M. Woerner, and T. Elsaesser, J. Chem. Phys. **130**, 164503 (2009).
[17] W. Kuehn, K. Reimann, M. Woerner, T. Elsaesser, and R. Hey, J. Phys. Chem. B **115**, 5448 (2011).
[18] K. Reimann, R. P. Smith, A. M. Weiner, T. Elsaesser, and M. Woerner, Opt. Lett. **28**, 471 (2003).
[19] The dimensionless IS dipole–LO dipole coupling strength η is measured in units of $\eta_0 = 4\ \mathrm{meV}/(e_0 \times 1\ \mathrm{nm})^2$.
[20] T. Kuhn, in *Theory of Transport Properties of Semiconductor Nanostructures*, edited by E. Schöll (Chapman & Hall, London, 1998), pp. 173–214.
[21] W. Kuehn *et al.*, Phys. Rev. Lett. **104**, 146602 (2010).